Supplement of Clim. Past, 18, 2483–2507, 2022
https://doi.org/10.5194/cp-18-2483-2022-supplement

Climate of the Past
Open Access
EGU

Supplement of

Leeuwin Current dynamics over the last 60 kyr – relation to Australian ecosystem and Southern Ocean change

Dirk Nürnberg et al.

Correspondence to: Dirk Nürnberg (dnuernberg@geomar.de)

Supplement

Introduction

The Supplement includes text passages, figures, and data tables supporting the abovementioned study. The text discusses in higher detail the ecology of the selected foraminiferal species, and diverse aspects relevant to the Mg/Ca-paleothermometry.

1. **Text S1** Supporting information on foraminiferal species selected and their ecology, analytical details and error assessment for foraminiferal Mg/Ca, contamination and calcite dissolution issues, chronostratigraphy, and references.
2. **Figure S1.** Contamination plots (core 2614)
3. **Figure S2.** Contamination plots (core 2609)
4. **Figure S3.** Downcore $Mg/Ca_{\textit{O.universa}}$ of core 2614
5. **Figure S4.** Downcore $Mg/Ca_{\textit{O.universa}}$ of core 2609
6. **Figure S5.** Downcore $Mg/Ca_{\textit{G.trunca}}$ of core 2609
7. **Figure S6.** Analytical results for western core 2614
8. **Figure S7.** Analytical results for eastern core 2609
9. **Figure S8.** Calculated Mg/Ca-based temperatures from western core 2614
10. **Figure S9.** Calculated Mg/Ca-based temperatures from eastern core 2609
11. **Figure S10.** Differently calculated SST records
12. **Figure S11.** ph-corrected $SST_{Mg/Ca}$ records (MgCaRB)
13. **Table S1.** Defined outliers
14. **Table S2.** Assessment of ph-effect on Mg/Ca: MgCaRB input parameters
15. **Table S3.** Radiocarbon datings

Text S1 Supporting information on foraminiferal species selected and their ecology, analytical details and error assessment for foraminiferal Mg/Ca, contamination and calcite dissolution issues, chronostratigraphy, and references.

Ecology, calcification depths, and seasonality of proxy formation

Planktonic foraminifera are marine protists living in the photic zone. They produce calcitic tests from calcium carbonate from the surrounding water. To reconstruct surface ocean conditions, we selected the near-surface species *Orbulina universa* (d'Orbigny, 1839). *O. universa* is a spinose planktonic foraminiferal species that inhabits surface waters throughout the tropical, subtropical and transition zones of the world ocean (Bé and Tolderlund, 1971). Early studies of their habitat preferences and morphology regard their morphotypes as belonging to the same genetic species, but showing phenotypic variations under different environmental conditions (Bé et al., 1973; Hecht et al., 1976; Colombo and Cita, 1980). These studies reveal that *O. universa* has a preference for dwelling within the photic zone between the surface mixed layer and the shallow thermocline, which is ~30-80 m water depth in our study areas (c.f. Fig. 2). *O. universa* has a 2-staged growth in their life cycle (Caron et al., 1987; Lea et al., 1995). In the juvenile stage, they build a multi-chambered trochospiral form covered with calcite spines. In the adult stage, they develop a final, large, spherical chamber that hosts 90-95 % of its total calcite (Spero and Parker, 1985). The final chamber continues to thicken until gametogenesis, during which their spines are shed (Hamilton et al., 2008).

Based on sediment trap studies, Deuser et al. (1981) proposed different calcification depths for different morphotypes of *O. universa*: thin-walled (5-10 μm) and thick-walled (up to 30 μm) morphotypes, with the thick-walled morphotypes secreting shells having ~0.5 ‰ higher $\delta^{18}O$ than the thin-walled variants. Marshall et al. (2015) pointed out that the different isotopic compositions of both morphotypes cannot be explained by seasonal variation, as they are both present year-round. For this study, we made no distinction between morphotypes, as both morphotypes of *O. universa* show resembling calcification depths (Anand et al., 2003; Farmer et al., 2007). The issue of a seasonal bias of proxies generated on *O. universa* is discussed further below.

To support the *O. universa* analytical results, we additionally analyzed *Globigerinoides ruber* white, which is a symbiont-bearing near surface dwelling species, living in the upper 50 m of the mixed layer (Bé and Hutson, 1977). It occurs in warmer regions, predominantly in subtropical regions. Several studies confirmed that *G. ruber* records reflect warmest water

conditions of the seasonal cycle (Regenberg, et al., 2009). Andrijanic (1988) showed omnipresent *G. ruber* in austral summer off the eastern Australian coast. We presume that *G. ruber* did not change habitat significantly over time, as it is a very shallow dwelling, symbiont-bearing species dependent on high light levels.

To reconstruct subsurface ocean properties, we selected calcitic tests of the planktonic foraminiferal species *Globorotalia truncatulinoides* (d´Orbigny, 1839). *G. truncatulinoides* is a deep-dwelling planktonic, subtropical species, which occurs over a broad range of water temperatures and salinities (e.g., Lohmann and Schweitzer, 1990; Ganssen and Kroon, 2000). For *G. truncatulinoides,* a coiling dimorphism is apparent, separating the species into left-coiled (sinistral) and right-coiled (dextral) morphotypes. The preferred habitats of both morphotypes, however, are rather similar (Jentzen et al., 2018; Cléroux et al., 2008). Friedrich et al. (2012) and Ganssen and Kroon (2000) found that both morphotypes have similar stable oxygen ($\delta^{18}O$) and carbon isotope ($\delta^{13}C$) compositions, and Mg/Ca signatures. We therefore made no distinctions between morphotypes.

G. truncatulinoides exhibits a complex life cycle, beginning in the upper meters of the water column in the photic zone. It continues to grow and calcify new chambers in deeper waters until it reaches the adult stage, thereby pursuing a reproductive strategy that requires annual vertical migration of several hundred meters, with greater living depths during spring and summer (Cléroux et al., 2009). Different encrustation stages of *G. truncatulinoides*, in this respect, may point to different calcification depths (Reynolds et al., 2018). In the Gulf of Mexico, non-encrusted and encrusted specimens reveal mean calcification depths of 66 ± 9 m (with a range between 0-150 m) and 379 ± 76 m (with a range between 170 and 700 m), respectively (Reynolds et al., 2018). As the majority of the *G. truncatulinoides* specimens in cores 2614 and 2609 are encrusted, we assume a rather deep habitat depth range.

Various studies reported that a higher abundance of *G. truncatulinoides* is associated with a very deep (permanent) thermocline and/or thick water thermostads (Lohmann and Schweitzer, 1990; Ravelo and Fairbanks, 1992; McKenna and Prell, 2004; Schiebel and Hemleben, 2005). In Tobago basin (tropical W-Atlantic), Nürnberg et al. (2021) assigned a calcification depth of ~200-250 m to *G. truncatulinoides*, which corresponds to a depth nearly below the main thermocline in this area. This notion is in good agreement with findings from the eastern Caribbean, where *G. truncatulinoides* apparently prefers a habitat at ~180-300 m (Jentzen et al., 2018). Cléroux et al. (2008) proposed that at mid-latitudes and high latitudes, the isotopic temperature of *G. truncatulinoides* exceeds winter temperatures, but coincide with summer temperatures around the base of the summer thermocline. In our study area, the base of the

summer thermocline is between ~350 and 400 m (Fig. 2), which is rather deep compared to other ocean areas.

Jonkers and Kučera (2015) projected that the flux pattern of the deep-dwelling *G. truncatulinoides* is rather regular over the year, with a high percentage of the annual flux occurring in a single high-flux pulse. For our derived $subSST_{Mg/Ca}$ records we reckon that the seasonal range at the base of the thermocline is minimal (Fig. 2), hence a seasonal bias for the proxy records, if any, is minimal.

Sample contamination

Marine sediment contains a significant proportion of clay (~1-10 % Mg by weight), which may perturb the foraminifereal Mg/Ca ratios, when tests are not cautiously cleaned prior to the analyses. By monitoring the foraminiferal samples for their Fe/Ca, Al/Ca and Mn/Ca ratios, the effect of cleaning efficiency, post depositional contamination, and diagenetic alteration on foraminiferal Mg/Ca was examined. Barker et al. (2003) and Them et al. (2015) proposed contamination-indicative threshold values for Fe/Ca, Al/Ca and Mn/Ca (<0.1 mmol mol^{-1}). Meanwhile, numerous studies have shown that these threshold values - defined in the North Atlantic - are often exceeded as they largely depend on the sediment type the foraminiferal tests were removed from (e.g. Nürnberg et al., 2021).

In many of our foraminiferal samples, the Al/Ca, Fe/Ca and Mn/Ca ratios are higher than the given threshold values, and at times reach values of up to ~0.7 mmol mol^{-1}, ~0.5 mmol mol^{-1}, and ~0.007 mmol mol^{-1}, respectively (Fig. S1; S2). Notably, these high contaminant values do not consistently have extremely high foraminiferal Mg/Ca ratios. Also, the correlation of $Mg/Ca_{O.universa}$ to either Al/Ca, Fe/Ca, or Mn/Ca for the core 2614 is insignificant (R^2= 0.0047, 0.0095 and 0.0497), suggesting that samples were not contaminated (Fig. S1). A high covariance between Mg/Ca and Mn/Ca, Fe/Ca and/or Al/Ca would imply insufficient clay removal during cleaning (Barker et al., 2003). Low correlation coefficients are also present in *O. universa* (R^2= 0.24, 0.32 and 0.14) and *G. truncatulinoides* samples from core 2609 (R^2= 0.62, 0.58 and 0.02) (Fig. S2).

In Figures S3–S5, the downcore comparison of Mg/Ca ratios to the contaminant element ratios Al/Ca, Fe/Ca and Mn/Ca are shown. From the comparisons, unusually high Mg/Ca ratios relative to contaminant element ratios were excluded from the downcore records, as they led to unrealistically high temperature estimates (Table S1).

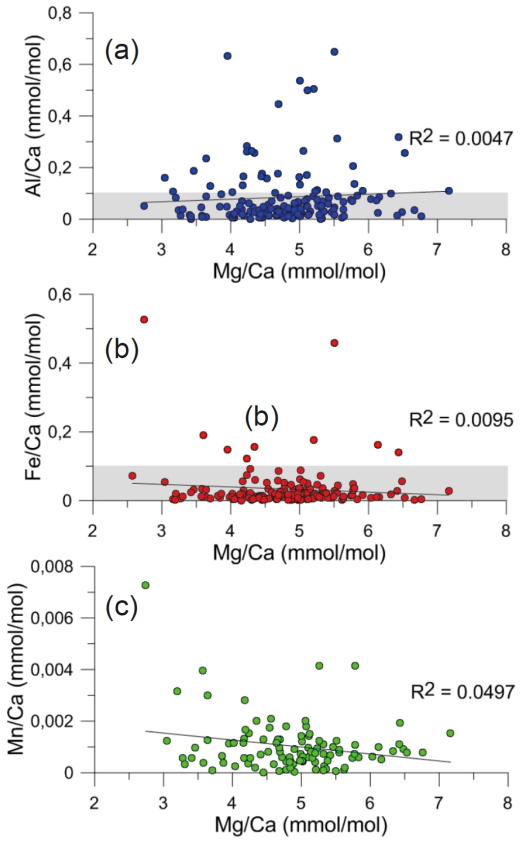

Figure S1. Contamination plots. Foraminiferal Mg/Ca vs. Al/Ca (a; blue), Fe/Ca (b; red) and Mn/Ca (c; green) for *O. universa* from core 2614. Al/Ca, Fe/Ca and Mn/Ca partly exceed threshold values (>0.1 mmol mol^{-1}, grey shading) proposed by Barker et al. (2003). R^2 = correlation coefficients.

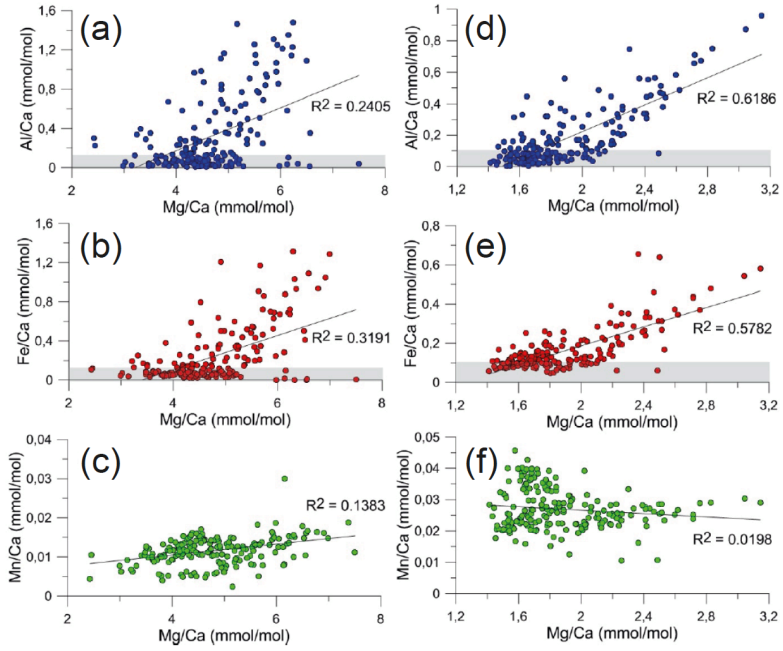

Figure S2. Contamination plots. Foraminiferal Mg/Ca vs. Al/Ca (blue), Fe/Ca (red) and Mn/Ca (green) for *O. universa* (left; a, b, c) and *G. truncatulinoides* (right; d, e, f) from core 2609. Al/Ca, Fe/Ca and Mn/Ca partly exceed threshold values (>0.1 mmol mol^{-1}, grey shading) proposed by Barker et al. (2003). R^2 = correlation coefficients.

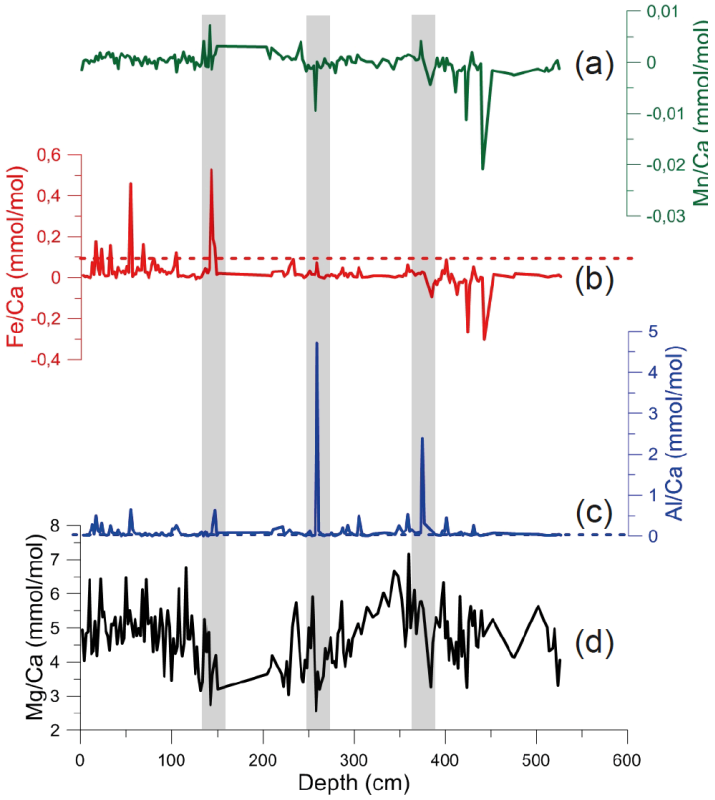

Figure S3. Downcore Mg/Ca$_{O.universa}$ of core 2614 (d) in comparison to contaminant elemental ratios Al/Ca (c), Fe/Ca (b), and Mn/Ca (a) from the same samples. Correlation coefficients are given in Figure S1. Threshold values provided by Barker et al. (2003) indicative of sample contamination (>0.1 mmol mol^{-1}) are indicated by the dashed lines, but should be viewed cautiously. Grey shaded bars mark the excluded samples (c.f. Table S1).

Table S1. Defined outliers with unusually high contaminant ratios taken out from further interpretations.

Core	Sample depth (cm)	Sample species	Mg/Ca (mmol mol^{-1})	Al/Ca (mmol mol^{-1})	Fe/Ca (mmol mol^{-1})	Mn/Ca (mmol mol^{-1})
2614	142	*O. universa*	2.74	0.05	0.53	0.007
	258		2.57	4.72	0.07	-0.009
	374		5.78	2.39	0.03	0.004
		G. trunca.	no data	no data	no data	no data
2609	64	*O. universa*	7.38	3.96	1.96	0.019
	166		4.92	2.22	1.21	0.08
	190		6.05	3.66	1.69	0.015
	26	*G. trunca.*	2.46	0.56	0.46	0.03
	52		3.04	0.87	0.54	0.03
	96		3.14	0.96	0.58	0.03

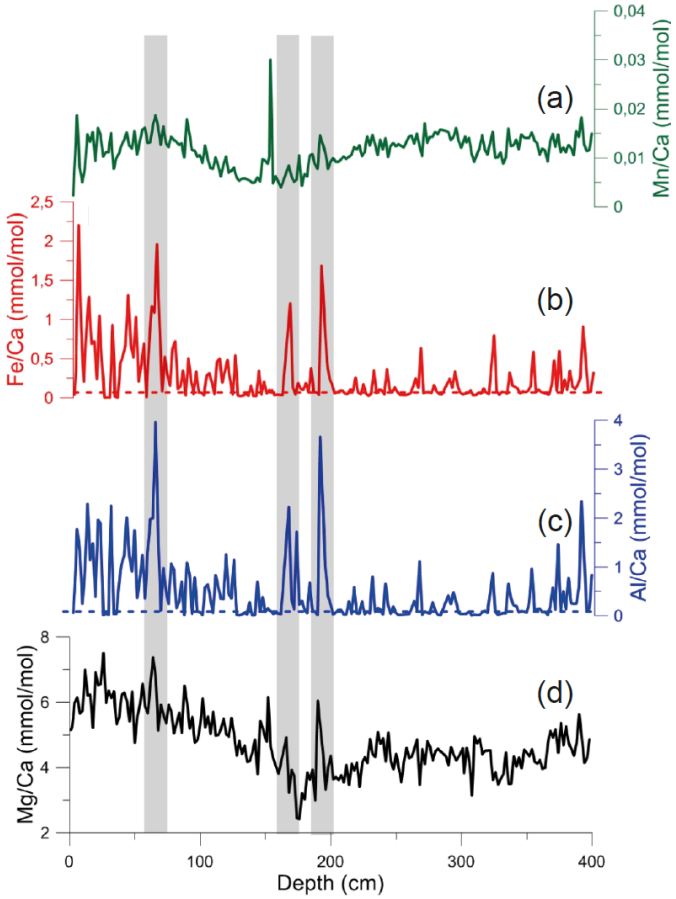

Figure S4. Downcore Mg/Ca*O.universa* of core 2609 (d) in comparison to contaminant elemental ratios Al/Ca (c), Fe/Ca (b), and Mn/Ca (a) from the same samples. Correlation coefficients are given in Figure S2. Threshold values provided by Barker et al. (2003) indicative of sample contamination (>0.1 mmol mol^{-1}) are indicated by the dashed lines, but should be viewed cautiously. Grey shaded bars mark the excluded samples (c.f. Table S1).

Calcite dissolution effects and preferential Mg-ion removal

Calcite dissolution in fact lowers foraminiferal Mg/Ca-based temperature estimates (e.g., Nürnberg et al., 1996; Regenberg et al., 2006). Nonetheless, many studies prove the large potential of the Mg/Ca-paleothermometry even in calcite-unsaturated waters (e.g., Nürnberg et al., 2015; Tapia et al., 2015). Approaches were introduced to correct for the Mg^{2+}-ion loss, either by correcting for water depth (e.g., Regenberg et al., 2006; Dekens et al., 2002) or by correcting for the degree of undersaturation with respect to calcite ion concentration (e.g., Regenberg et al., 2006; 2014). In the study area, the calcite saturation state $\Delta([CO_3^{2-}])$, which is the difference between the "*in situ*" carbonate ion concentration ($[CO_3^{2-}]$) and ($[CO_3^{2-}]$) at saturation, is 0 µmol kg^{-1} at >3700 m water depth today (Regenberg et al., 2006). The ~21.3 ± 6.6 µmol kg^{-1} threshold being considered as critical for selective Mg^{2+}-removal (Regenberg et al., 2006; 2014) is clearly shallower at ~1500 m water depth in the study area. While our western core 2614 from a water depth of 1070 m is above this critical threshold level, the

eastern core 2609 is ~500 m below this threshold level, making the dissolution-related perturbation of the Mg/Ca-signal possible. Nonetheless, the Holocene mean $SST_{Mg/Ca}$ and $subSST_{Mg/Ca}$ estimates appear close to the modern temperatures at the respective water depths (Fig. 2) suggesting that selective Mg^{2+}-ion removal due to calcite dissolution processes is rather negligible.

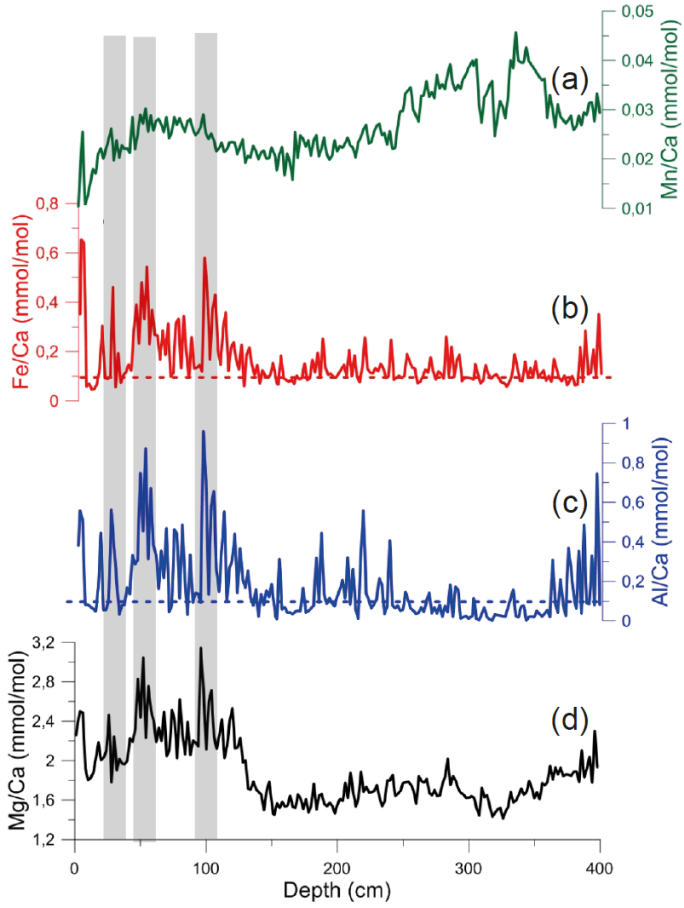

Figure S5. Downcore $Mg/Ca_{G.trunca}$ of core 2609 (d) in comparison to contaminant elemental ratios Al/Ca (c), Fe/Ca (b), and Mn/Ca (a) from the same samples. Correlation coefficients are given in Figure S2. Threshold values provided by Barker et al. (2003) indicative of sample contamination (>0.1 mmol mol^{-1}) are indicated by the dashed lines, but should be viewed cautiously. Grey shaded bars mark the excluded samples (c.f. Table S1).

Analytical results: Oxygen isotopes ($\delta^{18}O$) and Mg/Ca ratios

Western core 2614

The $\delta^{18}O_{G.ruber}$ record of core 2614 (van der Kaars et al., 2017) is rather similar to the $\delta^{18}O_{O.universa}$ record with respect to downcore variations and the deglacial amplitude change, although absolute $\delta^{18}O_{G.ruber}$ values are on average lighter by ~0.5 ‰. The $\delta^{18}O_{O.universa}$ record is generally lighter than the $\delta^{18}O_{G.trunca.}$ record, with $\delta^{18}O_{O.universa}$ showing a range between 0.1

and 1.5 ‰, while $\delta^{18}O_{G.trunca.}$ values are heavier ranging between 0.6 and 3.5 ‰ (Fig. S6). The species-specific $\delta^{18}O$-values hence, reflect the according living depths of the three species. The downcore variations in $Mg/Ca_{O.universa}$ are broadly reflected by $Mg/Ca_{G.ruber}$, although the amplitude fluctuations appear to be larger in $Mg/Ca_{O.universa}$. $Mg/C_{O.universa}$ is overall higher (~3-7.5 mmol mol^{-1}) than $Mg/Ca_{G.trunca.}$, (~0.8-5.2 mmol mol^{-1}) (Fig. S6). Notably, $Mg/Ca_{G.trunca.}$ exhibits various prominent excursions to extremely high values >4.5 mmol mol^{-1} and amplitudes of >4 mmol mol^{-1}.

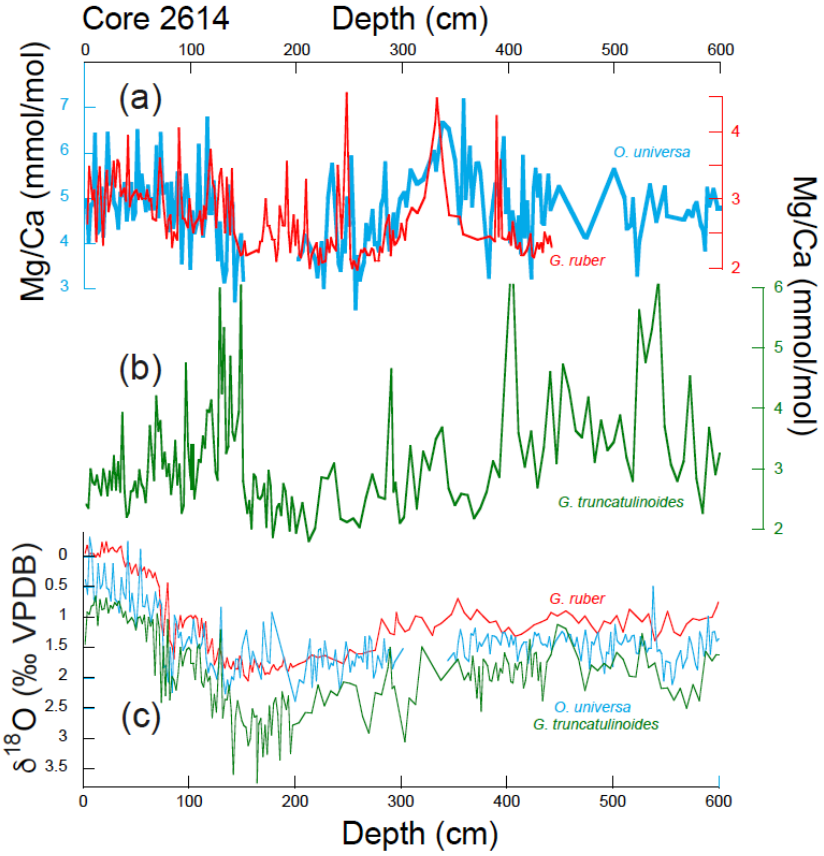

Figure S6. Analytical results for western core 2614. (a) Mg/Ca ratios of *G. ruber* (red), *O. universa* (blue) and (b) *G. truncatulinoides* (green). (c) Species-specific $\delta^{18}O$ records. The $\delta^{18}O_{G.ruber}$ data are from van der Kaars et al. (2017).

Eastern core 2609

Similar to core 2614, the absolute $\delta^{18}O$ values in the eastern core 2609 reflect the increasing calcification depths of the studied species, with $\delta^{18}O_{G.trunca.} > \delta^{18}O_{O.universa} > \delta^{18}O_{G.ruber}$. The $\delta^{18}O_{G.ruber}$ record is lighter by on average ~0.5 ‰ than the $\delta^{18}O_{O.universa}$ record, while their downcore amplitude variations are quite similar (Fig. S7). Both records are lighter by ~0.7-2 ‰ than the $\delta^{18}O_{G.trunca}$ record. Notably, the downcore $\delta^{18}O_{G.trunca}$ variations are larger than

those of the surface-dweller. They resemble those of core 2614, but are clearly heavier (Fig. S6).

The $Mg/Ca_{O.universa}$ and $Mg/Ca_{G.trunca.}$ records range between ~3-5-7 mmol mol^{-1}, and downcore variations are rather similar not exceeding ~2 mmol mol^{-1} (Fig. S7). The $Mg/Ca_{G.trunca.}$ record is on average ~4 mmol mol^{-1} lower than those of the shallow-dweller, and exhibits significantly lowered $Mg/Ca_{G.trunca.}$ below ~1.4 m core depth. Compared to core 2614, the core 2609 $Mg/Ca_{G.trunca.}$ record shows only small-scale amplitude variations of >1 mmol mol^{-1}.

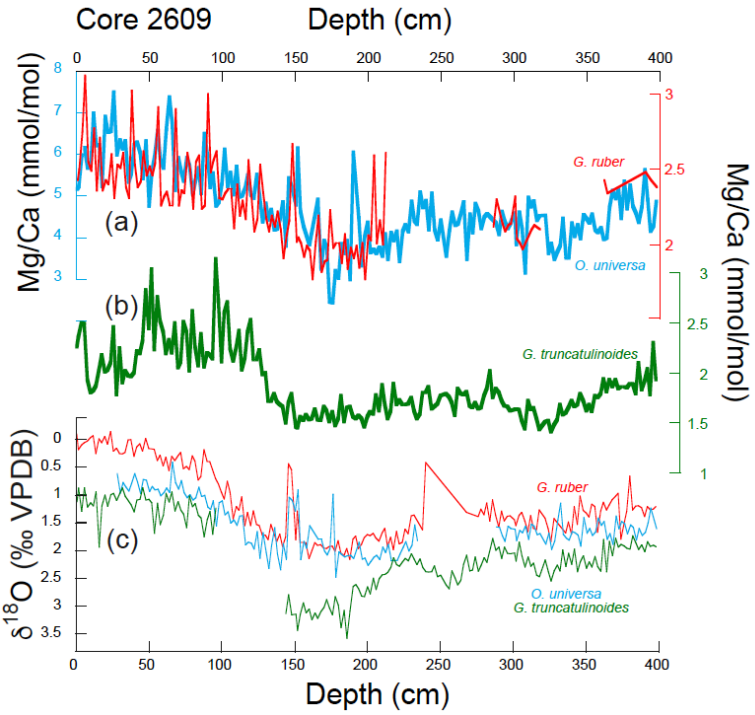

Figure S7. Analytical results for eastern core 2609. (a) Mg/Ca ratios of *G. ruber* (red), *O. universa* (blue) and (b) *G. truncatulinoides* (green). (c) Species-specific $\delta^{18}O$ records.

Foraminiferal Mg/Ca-paleothermometry

O. universa

The Mg/Ca ratios of *O. universa* were converted into sea surface temperatures ($SST_{Mg/Ca}$) using available species-specific temperature calibrations (c.f. Fig. S8, S9). We finally chose the calibration equation of Hathorne et al. (2003). This calibration function ($Mg/Ca = 0.95 \exp(0.086\ SST)$) is based on *O. universa* specimens recovered from a latitudinal transect in the North Atlantic to monitor their Mg-uptake. The calibration of Hathorne et al. (2003) provides a mean Holocene $SST_{Mg/Ca}$ of ~19.6° C in the western area, which is in broad agreement with the modern austral summer SST range in the upper thermocline/mixed layer (~30-80 m water depth) (Fig. S8, S9; c.f. Fig. 2). In the eastern area,

the same calibration provides a mean Holocene $SST_{Mg/Ca}$ of ~20.5° C, which exceeds the modern austral summer SST range. A discussion on this issue can be found in Chapter 4.3. The Russell et al. (2004) equation (Mg/Ca = 0.85 exp(0.096 SST)) provides results rather similar to the Hathorne et al. (2003) equation (Fig. S8). Other calibration functions from Lea et al. (1999), Anand et al. (2003a), and Regenberg et al. (2009) (Mg/Ca = 1.36 exp(0.085 SST); Mg/Ca = 0.38 exp(0.09 SST); Mg/Ca = 0.29 exp(0.101 SST)) provide either by several degrees too warm or too low SST-estimates.

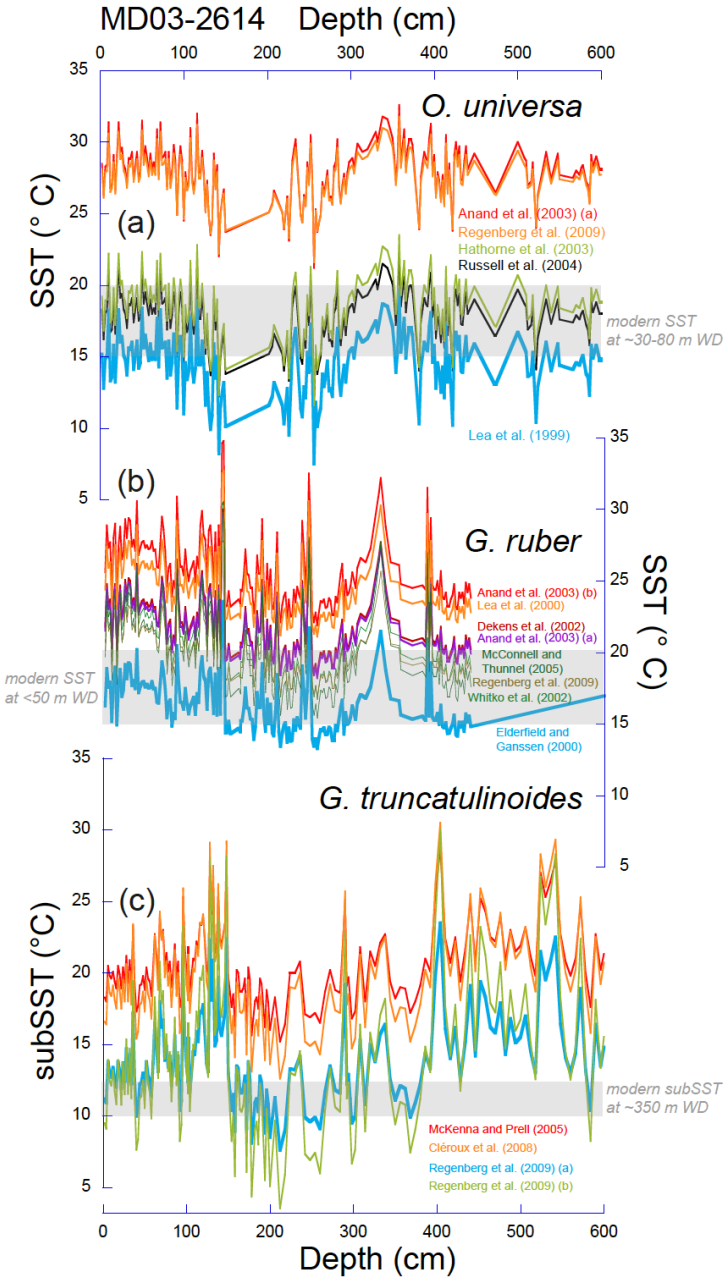

Figure S8. Calculated Mg/Ca-based temperatures from 0-600 cm core depth for western core 2614. The Mg/Ca data of *O. universa* (a), *G. ruber* (b), and *G. truncatulinoides* (c) were converted using species-specific temperature calibrations (c.f. legend). Modern annual SST at ~30-80 m, <50 m and ~350 m water depth are indicated (WOA, Locarnini et al., 2018), which are the most likely habitats of the studied species.

G. ruber

Although the Mg/Ca ratios of *G. ruber* follow in course and amplitude the according records of *O. universa*, and can be therefore taken as reliable support, we refrained from calculating $SST_{Mg/Ca}$ from Mg/Ca_{ruber} due to the following reasons: All temperature equations available for *G. ruber* (Lea et al., 2000: Mg/Ca = 0.30 exp (0.089 SST); Anand et al., 2003: Mg/Ca = 0.38 exp(0.09 SST), Mg/Ca = 0.342 exp(0.09 SST); Dekens et al., 2002: Mg/Ca = 0.37 exp(0.09(SST-0.36(core depth in km) - 2.0° C); McConnell and Thunnel et al., 2005: Mg/Ca = 0.69 exp(0.068 SST); Regenberg et al., 2009: Mg/Ca = 1.43 exp(0.047 SST); Whitko et al., 2002: Mg/Ca = 0.57 exp(0.074 SST)) provide SSTs, which are warmer by several degrees than the modern austral summer SST at <50 m water depth, and reach unrealistic paleo-SST of even >30° C in the western core 2614 (Fig. S8, S9). Only the Elderfield and Ganssen (2000) equation (Mg/Ca = 0.52 exp (0.10 SST)) provides a late Holocene $SST_{Mg/Ca}$, which comes close to the modern austral summer SST at <50 m water depth (15-16° C at core location 2609; 17-19° C at core location 2614). The core-top $SST_{Mg/Ca}$-estimates derived from *G. ruber* are hence, quasi equally warm than those of *O universa*. As the Elderfield and Ganssen (2000) equation, however, is a non-species-specific calibration but relies on various planktonic foraminiferal species, we assess this equation not applicable and hence, do not use the *G. ruber* proxy data for further interpretation.

G. truncatulinoides

The Mg/Ca ratios of the deep-dwelling *G. truncatulinoides* were converted into subsurface temperatures ($subSST_{Mg/Ca}$) using the calibration equation of Regenberg et al. (2009) (Mg/Ca = 1.32 exp(0.05 TT)). The Regenberg et al. (2009) study was based on calibrating Mg/Ca ratios of multiple planktonic foraminifera species (including *G. truncatulinoides*) obtained from (sub)tropical Atlantic sediment-surface samples with $\delta^{18}O$-derived calcification temperatures. The calibration provided Holocene $subSST_{Mg/Ca}$ estimates, which agree with the modern annual thermocline temperatures at the preferred depth of *G. truncatulinoides* in our study area (Fig. S8, S9). The error (standard deviation 2σ) is ±1.0° C. Other existing paleotemperature calibrations specific to *G. truncatulinoides* (e.g., McKenna and Prell, 2004: Mg/Ca = 0.355 exp(0.098 TT); Cléroux et al., 2008: Mg/Ca = 0.62 exp(0.074 TT); Regenberg et al., 2009: Mg/Ca = 0.84 exp (0.083 TT) and Mg/Ca = 1.32 exp (0.05 TT)) provide $TT_{Mg/Ca}$ estimates that are >7° C warmer than modern annual subsurface temperatures.

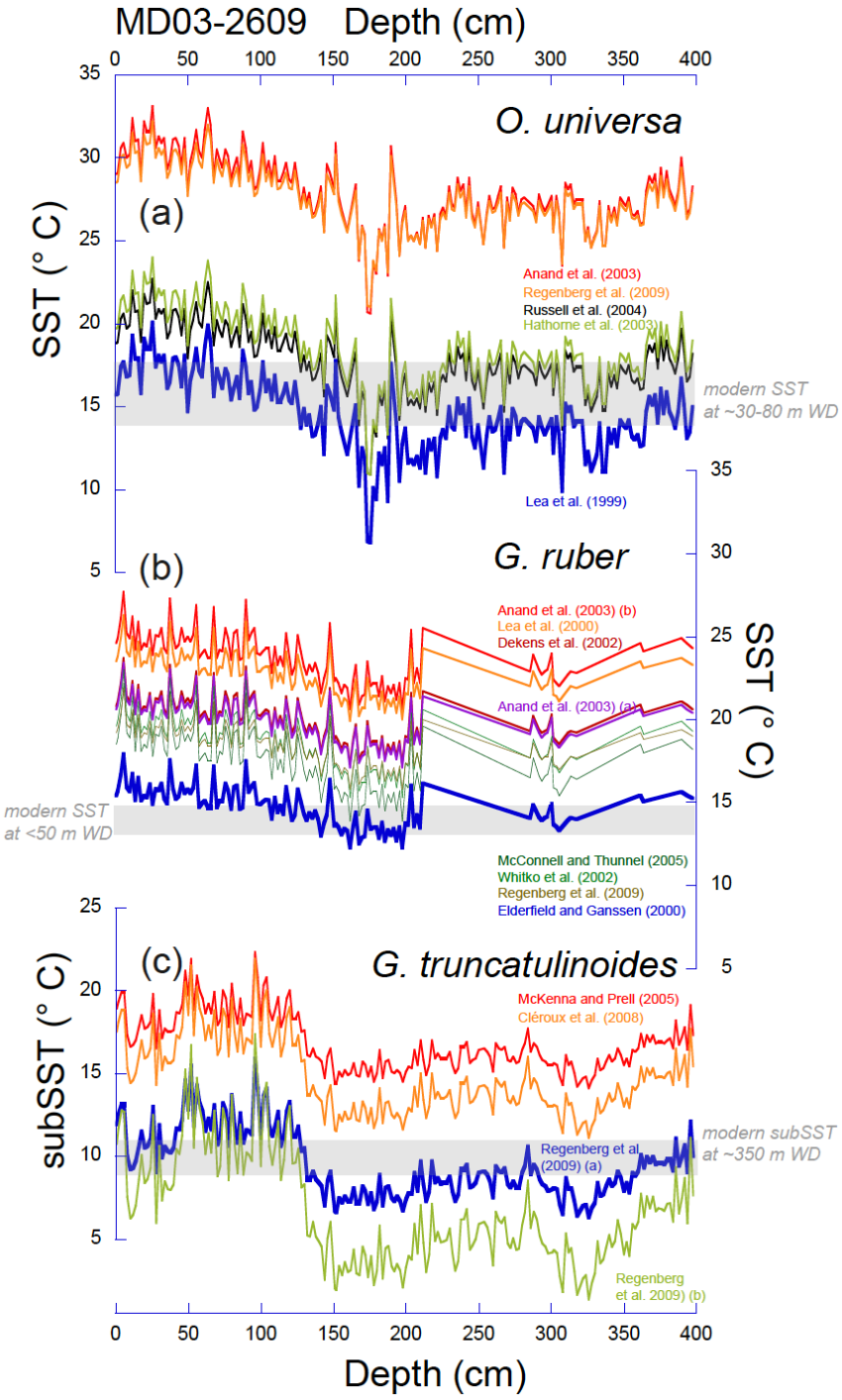

Figure S9. Calculated Mg/Ca-based temperatures from 0-400 cm core depth for eastern core 2609. The Mg/Ca data of *O. universa* (a), *G. ruber* (b) and *G. truncatulinoides* (c) were converted using species-specific temperature calibrations (c.f. legend). Modern annual SST at ~30-80 m, <50 m and ~350 m water depth are indicated (WOA, Locarnini et al., 2018), which are the most likely habitats of the studied species.

Growth seasonality is a relevant factor, which influences planktonic foraminiferal proxies and creates seasonal biases in the proxy signal recorded in a fossil assemblage (Jonkers and Kučera, 2015). The Holocene $SST_{Mg/Ca}$ estimates from the eastern core region are ~3-5° C warmer than the modern annual temperature range in the region. We take this as indication that the derived

$SST_{Mg/Ca}$ values represent the austral summer range during the Holocene. A seasonal bias for the reconstructed $TT_{Mg/Ca}$ records is considered minimal, although Jonkers and Kučera (2015) noted that the flux pattern of *G. truncatulinoides* is focused towards winter and spring. Overall, we presuppose that the habitat depths of the selected planktonic foraminifera are relatively stable through time.

pH-effect on foraminiferal Mg/Ca

Gray and Evans (2019) showed by culture experiments that the Mg/Ca-ratios of some planktonic species are sensitive to carbonate chemistry: Foraminiferal Mg/Ca declines with increasing pH (−5 to −9 % per 0.1 pH units). These results are mainly in accordance to earlier studies. Lea et al. (1999) claimed that seawater pH changes shell Mg/Ca by -6 % per 0.1 pH unit increase. Russell et al. (2004) stated: "Below ambient pH (pH < 8.2), Mg/Ca decreased by 7 ± 5 % (*O. universa*) to16 ± 6 % (*G. bulloides*) per 0.1 unit increase in pH. Above ambient pH, the change in Mg/Ca was not significant for either species (Russell et al., 2004)". Congruently, Kisakürek et al. (2008) found that the influence of pH on Mg/Ca ratios is negligible at ambient seawater pH (8.1 to 8.3). Below a seawater pH of 8.0, instead, pH has a dominating control on shell Mg/Ca. Hence, Russell et al. (2004) concluded that Mg/Ca-based paleotemperatures for the Quaternary, during which surface-ocean pH has been at or above modern levels, have not been biased by variations in surface-water pH.

The negative Mg/Ca vs. pH relationship is balanced by the fact that foraminiferal Mg/Ca is positively correlated with salinity: Nürnberg et al. (1996) already showed from culture experiments that Mg/Ca in *T. sacculifer* changes by 7-10 % per salinity unit. Lea et al. (1999) described a 4 ± 3 % change in Mg/Ca per salinity unit for *G. bulloides*, which is rather consistent to the 4 ± 3 % change per salinity unit for *G. ruber*. The Arbuszewski et al. (2010) study referred to an even higher salinity dependence (27 ± 4 %). Taken all data together, these results point to a strongly non-linear, positive salinity effect on shell Mg/Ca ratios.

Following Sanyal et al. (1995), who suggested an increase in salinity (by 1 unit) and pH (by 0.2 ± 0.1) in the oceans during the LGM, Lea et al. (1999) concluded that their opposing effects on shell Mg/Ca should partially cancel each other (also pointed out in Nürnberg, 2000).

Gray and Evans (2019) undertook new efforts in this respect. They claim that "the (pH) effect on Mg/Ca is considerably greater than that of salinity, resulting in a large bias in reconstructed temperature if unaccounted for... (Gray and Evans, 2019)". They presented the new software package "MgCaRB", which allows to correct foraminiferal Mg/Ca for pH down-core using

either atmospheric CO_2 or (preferably) boron isotopes (https://willyrgray.shinyapps.io/mgcarbv1/).

To better assess a possible bias of changed ocean pH on our reconstructed SST reconstructions off southern Australia, we applied the MgCaRB routines (Gray and Evans, 2019) to our Mg/Ca datasets. When using the program´s CO_2 approach, the relevant input parameters "modern salinity" and "modern alkalinity" where taken from the Ocean Data View (ODV) database from the respective core locations and species living depths (Table S2; Goyet et al., 2000). The resulting $SST_{Mg/Ca}$ records calculated with these modified salinity and alkalinity parameters (Table S2; grey and blue curves in Fig. S10) deviate within error for $SST_{Mg/Ca}$ estimates ($\pm$ ~1° C) from those calculated with the MgCaRB default settings. We hence consider these modifications of minor importance.

Table S2. For the assessment of the ph-effect on foraminiferal Mg/Ca, MgCaRB requires the input parameters "modern salinity", "modern alkalinity", and the assumed "modern pCO_2 disequilibrium" at the study sites. Modern salinity and alkalinity from the respective core locations and species living depths are from Goyet et al. (2000). For the modern pCO_2 disequilibrium, we tested 3 scenarios (see text).

	Habitat depth (m)	Salinity (psu)	Total alkalinity (µmol kg^{-1})	pCO_2 disequil. (µatm)	
MD03-2614	30-80	34.7	2288	-70 / 0 /+70	*O. universa*
34.7°S 123.4° E	350-400	34.6	2290	-70 / 0 /+70	*G. trunca.*
MD03-2609	30-80	34.7	2279	-70 / 0 /+70	*O. universa*
39.4°S 141.5° E	350-400	34.8	2286	-70 / 0 /+70	*G. trunca.*
MgCaRB default settings		35.0	2300	0	

MgCaRB offers 3 Mg/Ca vs. temperature calibrations, which might be applied to the *O. universa* Mg/Ca values. The "multispecies" calibration produces unreasonable $SST_{Mg/Ca}$ >24° C far above modern conditions and is hence not considered. The "generic calibration" provides $SST_{Mg/Ca}$, which are ~1-2° C cooler than those calculated with the "species-specific" calibration. Both calibrations provide core-top $SST_{Mg/Ca}$, which refer to austral winter SST. Instead, the Hathorne et al. (2003) calibration specifically established for *O. universa* and used in our study, provides warmer-by-3° C core-top $SST_{Mg/Ca}$, which is basically consistent with the austral summer SST in the area (see above why we opted for the calibration of Hathorne et al., 2003).

Notably, the MgCaRB-derived $SST_{Mg/Ca}$ records exhibit clearly cooler LGM conditions and higher amplitude variations (by 2-3° C) through time than the non-ph-corrected $SST_{Mg/Ca}$ record presented in our study (Fig. S10), which we assume less likely. Further, all MgCaRB calculations provide core-top (~1.3 ka BP) pH-estimates of ~8.18, which are definitely higher

than the modern surface ocean pH-value south of Australia (8.105-8.11; Gregor and Gruber, 2021; Raven et al., 2005). Downcore, the pH changes from 8.18 to 8.32 (at MgCaRB default settings). If Kisakürek et al. (2008) are correct, the influence of pH on Mg/Ca ratios in this pH-range is negligible.

For the deep-dwelling *G. truncatulinoides*, MgCaRB only offers the "multispecies" calibration, which produces unrealistic core-top $subSST_{Mg/Ca}$ values being higher-by-3-4° C than the modern subSST conditions. We hence will not continue to discuss the ph-corrected $subSST_{Mg/Ca}$ records.

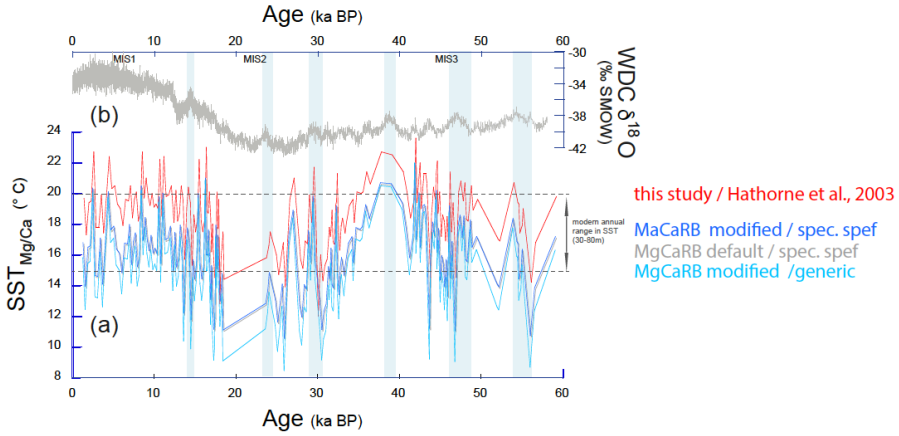

Figure S10. (a) Comparison of differently calculated SST records based on foraminiferal $Mg/Ca_{O.universa}$ from Site MD03-2614. Red: $SST_{Mg/Ca}$ record used in the manuscript, based on the Mg/Ca vs. T-relationship of Hathorne et al. (2003). Grey: $SST_{Mg/Ca}$ record calculated with MgCaRB using the default program settings and the *O. universa* species-specific calibration. Blue and light blue: $SST_{Mg/Ca}$ records calculated with MgCaRB using modified salinity and alkalinity settings (Table S1), and the species-specific (blue) and generic calibrations (light blue) for *O. universa*. (b) West Antarctic Ice Sheet Divide Core $\delta^{18}O$ record (WAIS Divide Project Members, 2015) as reference for the southern hemisphere climate signal.

In a further step, MgCaRB offers to include a value for the "modern pCO_2 disequilibrium" at the study site. The "modern pCO_2 disequilibrium" and its effect on the $SST_{Mg/Ca}$ estimates is difficult to assess due to the sparse database south of Australia. We first opted for the MgCaRB default setting of 0 µatm, pointing to equal pCO_2 concentrations in surface water and atmosphere. In a second step, we varied the pCO_2 disequilibrium conditions from -70 µatm (suggesting that the surface ocean is a CO_2-sink) to 70 µatm (surface ocean is a CO_2-source). These values are considered as reasonable endmember values for our evaluation (c.f. Takahashi et al., 2009). For the study area, in fact, monthly mean values for sea–air pCO_2 differences are clearly lower and range between ~-10 to ~-40 µatm (Takahashi et al., 2009) pointing to overall CO_2 absorbing (sink) conditions.

When applying MgCaRB, the more negative the pCO_2 disequilibrium is, the more positive will be the according $SST_{Mg/Ca}$ and pH estimates. Fig. S11 shows the core 2614 and core 2609 ph-corrected $SST_{Mg/Ca}$ records at the three different "modern pCO_2 disequilibrium" conditions outlined above: -70 µatm, 0 µatm (default), and +70 µatm. The according errors in $SST_{Mg/Ca}$ amount to on average ±0.9° C.

When assuming that the surface waters at the western Site 2614 originate mainly from tropical ocean areas (CO_2-source; releasing 0.5-1 mol C m^{-2} y^{-1}; McKinley et al., 2017; more positive pCO_2 disequilibrium; c.f. Takahashi et al., 2009; Greenop et al., 2017) while the eastern site is not, the western core would become even cooler at seasurface, thereby enhancing the $SST_{Mg/Ca}$ difference between the two sites. Instead at subsurface level: When assuming that the subsurface waters at the eastern Site 2609 are fed by subducted southern-sourced surface waters (CO_2-sink; absorbing CO_2 by -1 mol C m^{-2} y^{-1}; McKinley et al., 2017; more negative pCO_2 disequilibrium; c.f. Takahashi et al., 2009; Greenop et al., 2017), then the $subSST_{Mg/Ca}$ at the eastern location would likely become warmer, reducing the $subSST_{Mg/Ca}$ gradient to the western location. This effect is likely very small, as the deglacial ph of subantarctic surface water never fell below 8.0 (Shuttleworth et al., 2021), with almost negligible effects on foraminiferal Mg/Ca.

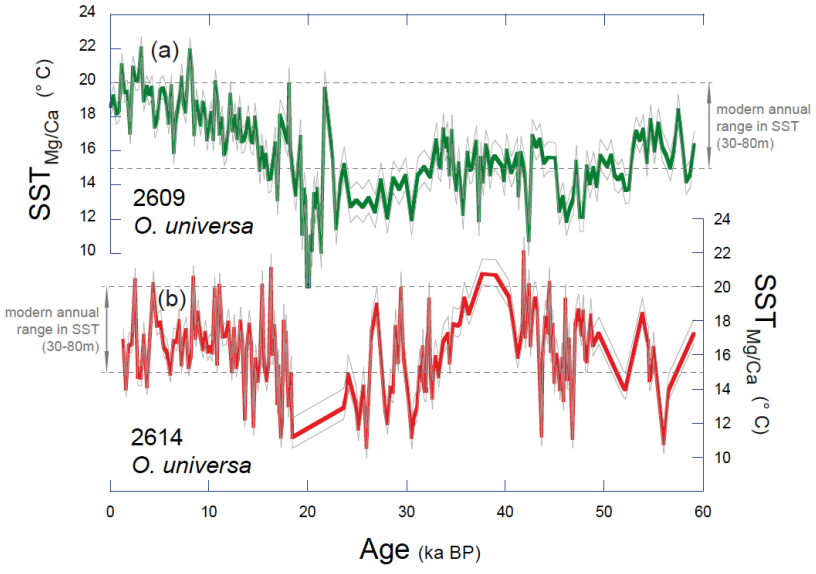

Figure S11. The core 2609 (a) and core 2614 (b) ph-corrected $SST_{Mg/Ca}$ records (using MgCaRB) at the three different "modern pCO_2 disequilibrium" conditions outlined above: -70 µatm (upper grey record), 0 µatm (red and green), and +70 µatm (lower grey record). The hatched lines mark the modern annual range in SST at 30-80 m water depth.

We cannot clarify all the issues raised by the Gray and Evans (2019) study, but our considerations imply that the ph-effect on our temperature reconstructions remains such small (<0.9° C; see above) that it has no major implication for our paleoceanographic interpretations. We note, instead, that it is the chosen Mg/Ca vs. temperature calibration, which is most crucial to our study. The choice of an inadequate (not regionally and species-specific calibrated) calibration equation may introduce errors. With respect to the warmer late Holocene $SST_{Mg/Ca}$ at the eastern site compared to the western site – which is basically opposite to what is initially expected from the modern situation - we give to consider that the late Holocene raw $Mg/Ca_{O.universa}$ ratios at the eastern site are undoubtedly higher than at the western location, affording a more differentiated interpretation.

Age model of sediment core MD03-2609 northwest of King Island.

The age model *of* core MD03-2609 is primarily based on the tuning of multiple planktonic $\delta^{18}O$ records to those of the well-dated reference core 2614 (van der Kaars et al., 2017). The tuning is further supported by 3 radiocarbon ($AMS^{14}C$) datings (Fig. 3; c.f. Table S3), for which a mix of shallow-dwelling planktonic foraminiferal tests was selected. The measurements were accomplished by Beta Analytic Radiocarbon Dating Laboratory, Florida, USA (info@betalabservices.com). All $AMS^{14}C$ dates were calibrated applying the BetaCal4.20 software, using the MARINE20 database. The marine calibration incorporates a time-dependent global ocean reservoir correction of ~ 550 ^{14}C yrs at 200 cal BP to ~410 ^{14}C yrs at 0 cal BP (Heaton et al., 2020). To account for local effects, the difference ΔR in reservoir age of the study area south of Australia and the model ocean was additionally considered. The Calib7.1 marine reservoir correction database provides a ΔR-value of -84 ± 65 years (Stuiver and Reimer, 1993).

Table S3. Radiocarbon ($AMS^{14}C$) datings performed on sediment core MD03-2609.

Core MD03-2609	Remark	Lab code	Sample type	^{14}C age raw	Age error	Calibrated median age	Age error	Reference
Depth (cm)				(yrs BP)	+/- (yrs)	(yrs BP)	+/- (yrs)	
164	$AMS^{14}C$	BETA-626880	mixed planktic	18610	60	19040	60	this study
230	$AMS^{14}C$	BETA-626881	mixed planktic	32530	230	32970	230	this study
304	$AMS^{14}C$	BETA-626882	mixed planktic	40820	530	41250	530	this study
314	$AMS^{14}C$	BETA-626883	mixed planktic	40820	520	41240	520	not considered

References

Andrijanic, S.: Geographical distribution of living planktonic foraminifera (Protozoa) off the east coast of Australia. Mar. Freshw. Res., 39 (1), 71–85, 1988.

Anand, P., Elderfield, H., and Conte, M.H.: Calibration of Mg/Ca thermometry in planktonic foraminifera from a sediment trap time series. Paleoceanography, 18 (2), 2003.

Arbuszewski, J., deMenocal, P., Kaplan, A., and Farmer, E.C.: On the fidelity of shell-derived $\delta^{18}O_{seawater}$ estimates. Earth Planet. Sci. Lett., doi:10.1016/j.epsl.2010.10.035, 2010.

Barker, S., Greaves, M., and Elderfield, H.: A study of cleaning procedures used for foraminiferal Mg/Ca paleothermometry. Geochem. Geophys. Geosystems, 4(9), 8407, doi:10.1029/2003GC000559, 2003.

Bé, A.W.H. and Tolderlund, D.S.: Distribution and ecology of living planktonic foraminifera in surface water of the Atlantic and Indian Oceans. Micropaleontol. Oceans, Cambridge University Press, London, 105-149, 1971.

Bé, A.W.H. and Hutson, W.H.: Ecology of planktonic foraminifera and biogeographic patterns of life and fossil assemblages in the Indian Ocean. Micropaleontology, 23, 369-414, 1977.

Bé, A.W.H., Harrison, S.M., and Lott, L.: *Orbulina universa* d'Orbigny in the Indian Ocean. Micropaleontology, 19, 150-192, 1973.

Caron, D.A.W., Faber, W., and Bé, A.W.H.: Growth of the spinose planktonic foraminifer *Orbulina universa* in laboratory culture and the effect of temperature on life processes. J. Mar. Biolog. Assoc. U.K., 67 (2), 343-358, 1987.

Cléroux, C., Cortijo, E., Anand, P., Labeyrie, L., Bassinot, F., Caillon, N., and Duplessy, J.-C.: Mg/Ca and Sr/Ca ratios in planktonic foraminifera: Proxies for upper water column temperature reconstruction. Paleoceanography, 23 (3), 2008.

Cléroux, C., Lynch-Stieglitz, J., Schmidt, M.W., Cortijo, E., and Duplessy, J.-C.: Evidence for calcification depth change of *Globorotalia truncatulinoides* between deglaciation and Holocene in the western Atlantic Ocean. Mar. Micropaleontol., 73, 57-61, 2009.

Colombo, M.R. and Cita, M.B.: Changes in size and test porosity of *Orbulina universa* d'Orbigny in the Pleisocene record of Cape Bojador (DSDP Site 397, eastern North Atlantic). Mar. Micropaleontol., 5, 13-29, 1980.

Dekens, P.S., Lea, D.W., Pak, D.K., and Spero, H.J.: Core top calibration of Mg/Ca in tropical foraminifera: Refining paleotemperature estimation. Geochem. Geophys. Geosystems, 3(4), 10.1029/2001GC000200, 2002.

Deuser, W.G., Ross, E.H., Hemleben, C., and Spindler, M.: Seasonal changes in species composition, numbers, mass, size and isotopic composition of planktonic foraminifera settling into the deep Sargasso Sea. Palaeoceanogr. Palaeoclimatol. Palaeoecol., 33, 103-127, 1981.

Elderfield, H. and Ganssen, G.: Past temperature and delta18O of surface ocean waters inferred from foraminiferal Mg/Ca ratios. Nature, 405 (6785), 442-445, 2000.

Farmer, E.C., Kaplan, A., de Menocal, P.B., and Lynch-Stieglitz, J.: Corroborating ecological depth preferences of planktonic foraminifera in the tropical Atlantic with stable oxygen isotope ratios of core-top specimens. Paleoceanography, 22, 1-14, 2007.

Friedrich, O., Schiebel, R., Wilson, P.A., Weldeab, S., Beer, C.J., Cooper, M.J., and Fiebig, J.: Influence of test size, water depth and ecology on Mg/Ca, Sr/Ca, $\delta^{18}O$ and $\delta^{13}C$ in nine modern species of planktic foraminifers. Earth Planet. Sci. Lett., 319-320, 133-145, 2012.

Ganssen, G. and Kroon, D.: The isotopic signature of planktonic foraminifera from NE Atlantic surface sediments: Implications for the reconstruction of past oceanic conditions. J. Geol. Soc. London, 157, 693-699, 2000.

Goyet, C, Healy, R, Ryan, J, and Kozyr, A.: Global Distribution of Total Inorganic Carbon and Total Alkalinity below the Deepest Winter Mixed Layer Depths. United States: N. p., doi:10.2172/760546, 2000.

Gray, W. R. and Evans, D.: Nonthermal influences on Mg/Ca in planktonic foraminifera: A review of culture studies and application to the last glacial maximum. Paleoceanogr. Paleoclimatol., 34, 306–315, https://doi.org/10.1029/2018PA003517, 2019.

Greenop, R., Hain, M.P., Sosdian, S.M., Oliver, K.I.C., Goodwin, P., Chalk, T.B., Lear, C.H., Wilson, P.A., and Foster, G.L.: A record of Neogene seawater $\delta^{11}B$ reconstructed from paired $\delta^{11}B$ analyses on benthic and planktic foraminifera. Clim. Past, 13, 149–170, doi:10.5194/cp-13-149-2017, 2017.

Gregor, L. and Gruber, N.: OceanSODA-ETHZ: a global gridded data set of the surface ocean carbonate system for seasonal to decadal studies of ocean acidification. Earth Syst. Sci. Data, 13, 777–808, https://doi.org/10.5194/essd-13-777-2021, 2021.

Hamilton, C.P., Spero, H.J., Bijma, J., and Lea, D.W.: Geochemical investigation of gametogenetic calcite addition in the planktonic foraminifera *Orbulina universa***.** Mar. Micropaleontol.*,* 68 (3), 256-267, 2008.

Hathorne, E.C., Alard, O., James, R.H., and Rogers, N.W.: Determination of intratest variability of trace elements in foraminifera by laser ablation inductively coupled plasma-mass spectrometry. Geochem. Geophys. Geosystems*,* 4(12), 8408, doi:10.1029/2003GC000539, 2003.

Heaton, T.J., Köhler, P., Butzin, M., Bard, E., Reimer, R.E., Austin, W.E.N., Bronk Ramsey, C., Grootes, P.M., Hughen, K.A., Kromer, B., Reimer, P.J., Adkins, J., Burke, A., Cook, M.S., Olsen, J., and Skinner, L.C.: MARINE20 – The marine radiocarbon age calibration curve (0–55,000 CAL BP). Radiocarbon, 62 (4), 779–820, DOI:10.1017/RDC.2020.68, 2020.

Hecht, A.D., Bé, A.W.H., and Lott, L.: Ecologic and paleoclimatic implications of morphologic variation of *Orbulina universa* in the Indian Ocean. Science*,* 194, 422-424, 1976.

Jentzen, A., Nürnberg, D., Hathorne, E.C., and Schönfeld, J.: Mg/ Ca and $\delta^{18}O$ in living planktic foraminifers from the Caribbean, Gulf of Mexico and Florida Straits. Biogeosciences, 15 (23), 7077–7095, https://doi.org/10.5194/bg-15-7077-2018, 2018.

Jonkers, L. and Kucera, M.: Global analysis of seasonality in the shell flux of extant planktonic foraminifera. Biogeosciences*,* 12 (7), 2207-2226, 2015.

Kisakürek, B., Eisenhauer, A., Böhm, F., Garbe-Schönberg, D., and Erez, J.: Controls on shell Mg/Ca and Sr/Ca in cultured planktonic foraminifera, *Globigerinoides ruber* (white). Earth Planet. Sci. Lett., 273, 260–269, doi:10.1016/j.epsl.2008.06.026, 2008.

Lea, D.W., Martin, P.A., Chan, D.A., and Spero, H.J.: Calcium uptake and calcification rate in the planktonic foraminifer *Orbulina universa*. J. Foram. Res., 25, 185-206, 1995.

Lea, D.W., Mashiotta, T.A., and Spero, H.J.: Controls on magnesium and strontium uptake in planktonic foraminifera determined by live culturing. Geochim. Cosmochim. Acta, 63 (16), 2369-2379, 1999.

Lea, D.W., Pak, D.K., and Spero, H.J.: Climate impact of Late Quaternary equatorial Pacific sea surface temperature variations. Science*,* 289, 1719-1724, 2000.

493 Locarnini, R.A., Mishonov, A.V., Baranova, O.K., Boyer, T.P., Zweng, M.M., Garcia, H.E., Reagan, J.R., Seidov,
494 D., Weathers, K.W., Paver, C.R., and Smolyar, I.V.: Temperature. NOAA Atlas NESDIS, in: World Ocean
495 Atlas 2018 (1), edited by Levitus, S., 2018.
496 Lohmann, G.P. and Schweitzer, P.N.: *Globorotalia truncatulinoides'* growth and chemistry as probes of the past
497 thermocline: 1. Shell size. Paleoceanogr. Paleoclimatol., 5 (1), 55-75,
498 https://doi.org/10.1029/PA005i001p00055, 1990.
499 Marshall, B.J., Thunell, R.C., Spero, H.J., Henehan, M.J., Lorenzoni, L., and Astor, Y.: Morphometric and stable
500 isotopic differentiation of *Orbulina universa* morphotypes from the Cariaco Basin, Venezuela. Mar.
501 Micropaleontol., 10.1016/j.marmicro.2015.08.001, 2015.
502 McConnell, M.C. and Thunell, R.C.: Calibration of the planktonic foraminiferal Mg/Ca paleothermometer:
503 Sediment trap results from the Guaymas Basin, Gulf of California. Paleoceanography, 20, PA2016,
504 doi:10.1029/2004PA001077, 2005.
505 McKenna, V.S. and Prell, W.L.: Calibration of the Mg/Ca of *Globorotalia truncatulinoides* (R) for the
506 reconstruction of marine temperature gradients. Paleoceanography, 19 (2),
507 https://doi.org/10.1029/2000PA000604, 2004.
508 McKinley,G.A., Fay, A.R., Lovenduski, N.S., and Pilcher, D.J.: Natural Variability and Anthropogenic Trends in
509 the Ocean Carbon Sink. Ann. Rev. Mar. Sci., 9, 125–50, doi:10.1146/annurev-marine-010816-060529, 2017.
510 Nürnberg, D.: Taking the temperature of past ocean surfaces. Science, 289, 1698-1699, 2000.
511 Nürnberg, D., Bijma, J., and Hemleben, C.: Assessing the reliability of magnesium in foraminiferal calcite as a
512 proxy for water mass temperatures. Geochim. Cosmochim. Acta, 60 (5), 803-814, 1996.
513 Nürnberg, D., Riff, T., Bahr, A., Karas, C., Meier, K. and Lippold, J.: Western boundary current in relation to
514 Atlantic Subtropical Gyre dynamics during abrupt glacial climate fluctuations. Glob. Planet. Change, 201, doi:
515 10.1016/j.gloplacha.2021.103497, 2021.
516 Ravelo, A.C. and Fairbanks, R.G.: Oxygen isotopic composition of multiple species of planktonic foraminifera:
517 Recorders of the modern photic zone temperature gradient. Paleoceanography, 7, 815-831, 1992.
518 Raven et al.: Ocean acidification due to increasing atmospheric carbon dioxide. The Royal Society. ISBN 0 85403
519 617 2, www.royalsoc.ac.uk, 2005.
520 Regenberg, M., Nürnberg, D., Steph, S., Groeneveld, J., Garbe-Schönberg, D., Tiedemann, R., and Dullo, W.C.:
521 Assessing the effect of dissolution on planktonic foraminiferal Mg/Ca ratios: Evidence from Caribbean core
522 tops. Geochem. Geophys., Geosystems, 7(7), Q07P15, doi:10.1029/2005GC001019, 2006.
523 Regenberg, M., S. Steph, D. Nürnberg, R. Tiedemann, and Garbe-Schönberg, D.: Calibrating Mg/Ca ratios of
524 multiple planktonic foraminiferal species with δ^{18}O-calcification temperatures: Paleothermometry for the upper
525 water column. Earth Planet. Sci. Lett., *278*(3), 324-336, 2009.
526 Regenberg, M., Regenberg, A., Garbe-Schönberg, D., and Lea, D.W.: Global dissolution effects on planktonic
527 foraminiferal Mg/Ca ratios controlled by the calcite-saturation state of bottom waters. Paleoceanography, 29
528 (3), 127–142, 2014.
529 Reynolds, C.E, Richey, J.N., Fehrenbacher, J.S., Rosenheim, B.E., and Spero, H.J.: Environmental controls on
530 the geochemistry of *Globorotalia truncatulinoides* in the Gulf of Mexico: Implications for paleoceanographic
531 reconstructions. Mar. Micropaleontol., 142, 92–104, https://doi.org/10.1016/j.marmicro.2018.05.006, 2018.

Russell, A.D., Hönisch, B., Spero, H.J., and Lea, D.L.: Effects of seawater carbonate ion concentration and temperature on shell U, Mg, and Sr in cultured planktonic foraminifera. Geochim. Cosmochim. Acta, 68 (21), 4347–4361, doi:10.1016/j.gca.2004.03.013, 2004.

Sanyal, A., Hemming, N.G., Hanson, G.N., and Broecker, W.S.: Evidence for a higher pH in the glacial ocean from boron isotopes in foraminifera. Nature, 373 (6511), 234–236, 1995.

Schiebel, R. and Hemleben, Ch.: Modern planktic foraminifera. Palaontol. Z., 79 (1), 135–148, 2005.

Shuttleworth, D., Bostock, H.C., Chalk, T.B., Calvo, E., Jaccard, S.L., Pelejero, C., Martinez-Garcia, A., and Foster, G.L.: Early deglacial CO_2 release from the Sub-Antarctic Atlantic and Pacific oceans. Earth Planet. Sci. Lett., 554, 116649, https://doi.org/10.1016/j.epsl.2020.116649, 2021.

Spero, H.J. and Parker, S.L.: Photosynthesis in the symbiotic planktonic foraminifera *Orbulina universa*, and its potential contribution to oceanic primary productivity. J. Foraminifera. Res., 15, (4), 273-281, 1985.

Stuiver, M. and Reimer, P.J.: CALIB rev. 8. Radiocarbon, 35, 215-230, 1993.

Takahashi, T., Sutherland, S.C., Wanninkhof, R., Colm Sweeney, C., Feely, R.A., Chipman, D.W., Hales, B., Friederich, G., Chavez, F., Sabine, C., Watson, A., Bakker, D.C.E, Schuster, U., Metzl, N., Yoshikawa-Inoue, H., Ishii, M., Midorikawa, T., Nojiri, Y., Körtzinger, A., Steinhoff, T., Hoppema, M., Olafsson, J., Arnarson, T.S., Tilbrook, B., Johannessen, T., Olsen, A., Bellerby, R, Wong, C.S., Delille, B., Bates, N.R., and de Baar, H.J.W.: Climatological mean and decadal change in surface ocean pCO_2, and net sea–air CO_2 flux over the global oceans. Deep Sea Res. Part II, 56, 554–577, doi:10.1016/j.dsr2.2008.12.009, 2009.

Tapia, R., Nürnberg, D., Ronge, T., and Tiedemann, R.: Disparities in glacial advection of Southern Ocean Intermediate Water to the South Pacific Gyre. Earth Planet. Sci. Lett., 410, 152–164, http://dx.doi.org/10.1016/j.epsl.2014.11.031, 2015.

Them, T.R., Schmidt, M.W., and Lynch-Stieglitz, J.: Millennial-scale tropical atmospheric and Atlantic Ocean circulation change from the last Glacial Maximum and Marine Isotope Stage 3. Earth Planet. Sci. Lett., 427, 47–56, 2015.

Whitko, N., Hastings, D.W., and Flower, B.P.: Past sea surface temperatures in the tropical South China Sea based on a new foraminiferal Mg calibration, J. Mar. Sci., 1, doi:MARSci.2002.01.020101, 2002.

van der Kaars, S., Miller, G.H., Turney, C.S.M., Cook, J.E., Nürnberg, D., Schönfeld, J., Kershaw, A.P., and Lehman, S.J.: Human rather than climate the primary cause of Pleistocene megafaunal extinction in Australia. Nat. Commun., 8, 14142, https://doi.org/10.1038/ncomms14142, 2017.